The Orbit of Asteroid 2000 JQ66

Written 7/30/2016

Stanley Yu, Christina Jung, and Bryan Portillo

Summer Science Program 2016 at CU Boulder
Sommers-Bausch Observatory, Boulder, CO, USA 80305

e-mail address: stanley93yu@gmail.com, chrissyjung98@gmail.com, bryanportillo2772@gmail.com

This paper researches and determines the orbit of the near-Earth asteroid 2000 JQ66. Beginning by processing images collected from a 1301E CCD camera through a least-squares plate reduction program, we compute an accurate value for the RA and declination at three different observation times. Using this data, the classical orbital elements are determined and tested for precision through uncertainty measuring techniques, like ephemeris checks and "jackknifing." The orbital elements determined were: semi-major axis=2.164660±0.004523 AU; eccentricity=0.4186375±0.0004642; inclination=7.084588±0.02865 deg; longitude of ascending node=189.1004±0.4818 deg; argument of perihelion=103.5142±0.4787; mean anomaly=5.538538±0.9752.

INTRODUCTION

Asteroids are small, inactive bodies of rock and metals such as iron, nickel, and cobalt that are usually originated from the inner Solar System but not entirely. Asteroids range from sizes as small as pebbles to as big as 950. kilometers in diameter such as Ceres, to the point of being classified as a dwarf planet. Meteorites found on Earth are often from asteroids and are used to study asteroids such as in their composition. As shown in Figure 1, the first asteroid was found in 1801 by Giuseppe Piazzi and was originally classified as a planet. After its orbit was better defined, Piazzi named it Ceres after the Roman goddess of agriculture [1]. This discover sparked observations to be made to locate similar objects in the celestial sphere. By the end of the nineteenth century, there were several hundred asteroids discovered and recorded. Today, there are millions of asteroids discovered and being tracked and researched , however there are millions of others that are too small to be seen from the Earth.

FIGURE 1. Ceres is the largest asteroid in the asteroid belt. Discovered on 1 January 1801 by Giuseppe Piazzi, it was originally considered a planet. Several similar objects were located nearby and as result, Ceres was reclassified as an asteroid in the 1850s.

Moreover, asteroids are classified by their position in the solar system.[1] Main Belt asteroids are located between about two to four AU distance from the Sun, basically known as the asteroid belt. A near-Earth asteroid is a small asteroid whose orbit brings it exceedingly ambient to the Earth's. Figure 2 shows the relative location of most of the asteroids in the solar system. The majority of

asteroids are located within the asteroid belt. These orbits have a really low-eccentricity so their orbits are not very elongated. Asteroids are more numerous than thought. The ISO Deep Asteroid Search has indicated that there are over 1.1 million asteroids larger than 1 kilometer in the main asteroid belt. [3] This value is twice as scientists have previously predicted.

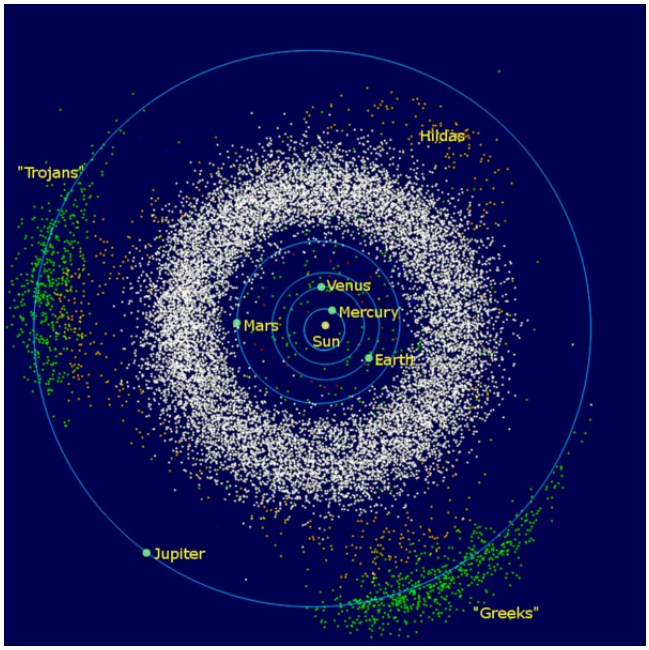

FIGURE 2. The inner Solar System is shown from the Sun to Jupiter's orbit. The densest part is the asteroid belt (depicted in white). Even though Earth is not as close to the asteroid belt with comparison to Mars, several asteroids are located near earth and may cross orbits with the planet.

Purpose

Everyday, the Earth is bombarded by asteroids, over 100 tons of dust and sand-sized particles. [4] Asteroids are always attacking the Earth, however our atmosphere burns up most of the asteroids before they reach the ground. As seen in Figure 3, when a small meteor enters the Earth's atmosphere, it's forced through the atmosphere. The meteor causes the air in front of the asteroid to compress. The temperature rises and burns the meteor until nothing is left. There are millions of asteroids in our solar system that are believed to be remains of planet formation from our early solar system from more than four billion years ago. [5] For these reasons, an asteroid that make it past the atmosphere will cause damage to the area hit . The larger impact is, the range of its effects are also larger on the Earth.

FIGURE 3. As asteroids enter the atmosphere and burn up, they leave a streak of light. Objects such as this asteroid disintegrate relatively fast as they ram at high speeds through the atmosphere.

A near-Earth asteroid is a small asteroid whose orbit brings it exceedingly ambient to the Earth's. Such asteroids could potentially strike the Earth and produce a considerable amount of casualty to the Earth as asteroid collisions have been culprits of dynamic alterations in the biological and ecological account of the Earth.

Our Research

Data of near-Earth asteroids such as of 2000 JQ66 are taken over a course of a few weeks at three or more different observations in order to calculate its orbit and see if eventually this asteroid will collide with Earth and overall, provide humanity with an admonitory to prevent or skew an Earth-asteroid collision. Our use of an 18" Cassegrain telescope determined the location of 2000 JQ66 at three separate locations in the celestial sphere. Using this data, the asteroid's orbital elements were calculated. In this paper, we examine and analyze the orbital pattern of 2000 JQ66 and understand whether its orbit will deviate as a result of Gravitational forces from nearby planets such as the Earth. From these results, we can ultimately find the asteroid's orbit.

METHODS

Data Collection

The images of 2000 JQ66 were taken on the 18'' Cassegrain Telescope at Sommers-Bausch Observatory (Figure 4) over the period of July 14th, 2016 to July 27th, 2016. Prior to each observation, observation notebooks

were completed with the ephemeris obtained from JPL's Horizon system and a star chart generated with the USNO Image and Catalog website, both of which helped us locate the asteroid. Three sets of five images were taken during each 2 hour observing session with 180 seconds exposure time.

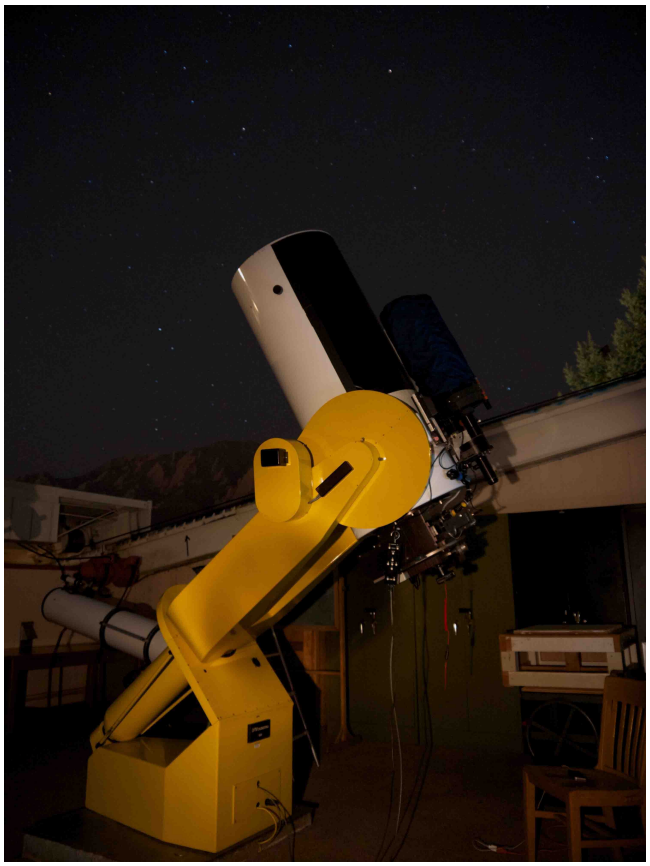

FIGURE 4. An image of the 18" telescope at Sommers-Bausch Observatory used to collect data for 2000 JQ66. Attached to the telescope is the 1301E CCD camera, which captured the photons from the sky and reads them into an image.

Procedures and Algorithms

Among the collected data, we chose the images taken on July 15th, 2016 7:00-9:00 UTC, July 23rd, 2016 5:00-7:00 UTC, and July 27th 5:00-7:00 UTC. The 15 images taken on each observing session were aligned and animated to locate the asteroid. Then, from one image per observing session (refer to Results section for images), the right ascension, declination, x-coordinate, and y-coordinate of 6 reference stars along with the x and y coordinates of our asteroid were obtained through SAO DS9. The values were then run through the Centroid and LSPR program (refer to Programs section below) to generate the right ascension and declination of the asteroid (Appendix 1). In order to estimate the magnitude of our asteroid to present to the Minor Planet Center at the Smithsonian Astrophysical Observatory, flat field corrections were applied to the images using Maxim DL. We input the R magnitude of a star of known magnitude, then had the program read out the magnitude of the asteroid. The right ascension, declination, and time of observation were run through the Orbit Determination program to generate of the position and velocity vectors along with the orbital elements.

To determine the orbit of an asteroid, the orbital elements need to be calculated from the r_0 and $\dot{r}_0$ vectors. Six orbital elements are necessary to fully determine the orbit of the asteroid (Figure 5), and they consist of the following: semi-major axis, eccentricity, inclination, longitude of ascending node, argument of perihelion, and mean anomaly.

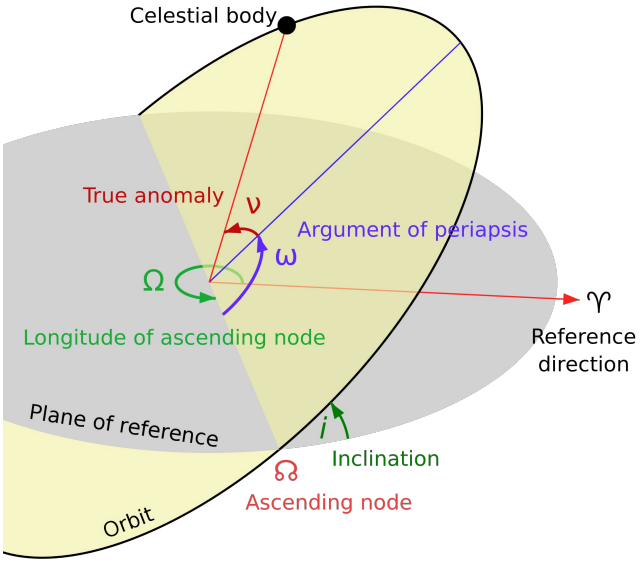

FIGURE 5. A diagram depicting the orbital plane and plane of reference for an asteroid. The classical orbital elements are included in the diagram to indicate the components required to completely and quantitatively describe an asteroid's orbit.

Programs

The Centroid and Least Squares Plate Reduction (LSPR) program processes the image and reference star data. The centroid of the reference star and asteroid is determined by measuring pixel counts, and the best-fit plate coefficients

are calculated for an estimation of residuals and standard deviation of the star and asteroid positions as well as their magnitudes. Based on the calculated values, the program determines the right ascension and declination of the asteroid and the uncertainty with the calculated coefficients using the following formulas:

$$\alpha = b_1 + a_{11}x + a_{12}y$$
$$\delta = b_2 + a_{21}x + a_{22}y$$

The Orbit Determination program reads in three observations from a file in the format of time(Julian days), right ascension(decimal hours), declination(decimal degrees), and the x, y, z-components of the sun vector(AU) for each observation obtained from JPL Horizons. The position and velocity vectors of the asteroid at the middle observation time are calculated using the Method of Gauss, and three terms were used in the f and g series (refer to Appendix 2 for details). The program finally outputs the vector orbital elements, the light-corrected time for the middle observation, and the classical orbital elements. Using the f and g series values, the vector orbital elements can be computed iteratively with the following formula:

$$\vec{r_0} = \frac{g_{+1}\vec{r_{-1}} - g_{-1}\vec{r_{+1}}}{f_{-1}g_{+1} - f_{+1}g_{-1}}$$

$$\dot{\vec{r_0}} = \frac{f_{+1}\vec{r_{-1}} - f_{-1}\vec{r_{+1}}}{f_{+1}g_{-1} - f_{-1}g_{+1}}$$

The Ephemeris Generation program takes in as input the eccentricity, semi-major axis, inclination, longitude of the ascending node, Argument of Perihelion, time of perihelion, and the time of observation. Using the input values, the Cartesian coordinates of the asteroid's position vector is calculated so that the x axis coincides with perihelion. Then the position vector is rotated by the argument of perihelion, inclination, and longitude of the ascending node to generate the r vector in ecliptic coordinates, which is converted to equatorial coordinates by rotating by the tilt of the earth relative to the ecliptic. With the earth sun vector obtained from JPL Horizons and the calculated r vector, the program solves for the right ascension and declination.

RESULTS

The right ascension, declination, time of observation, magnitude, and orbital elements of our asteroid as collected from our images are presented below.

From Appendix 1:

	Right Ascension (hms, dec)	Declination (dms, dec)	Time (UT, JD)	Mag	SNR
#1	21 33 43.051 21.56227	+13 46 50.90 13.80992	07/15/08:20:01 2457584.83333	17.3	24
#2	21 43 19.613 21.73562	+13 53 13.93 13.81452	07/23/06:27:31 2457592.75002	17.0	27
#3	21 48 29.012 21.80834	+13 32 31.01 13.48258	07/27/05:56:24 2457596.75001	17.0	26

TABLE 1. A table showing the results of our three asteroid observations with right ascension (Epoch 2000.0) in both hms and decimal degrees, declination (Epoch 2000.0) in both dms and decimal degrees, time in both month/day/UT and Julian days, a magnitude estimate to the tenth of a magnitude, and a signal-to-noise ratio value. The asteroid data was submitted to the Minor Planet Center at the Smithsonian Astrophysical Observatory.

The data calculations above were based on the images below, taken on July 15th, 2016 08:20:01 UTC, July 23rd, 2016 06:27:31 UTC, and July 27th, 2016 05:26:40 UTC respectively.

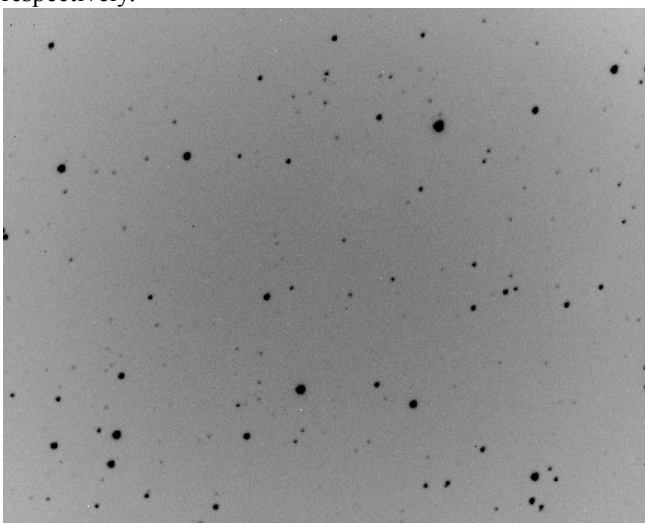

FIGURE 6. Image of 2000 JQ66 on July 15th, 2016 08:20:01 UTC taken with a 180 second exposure time.

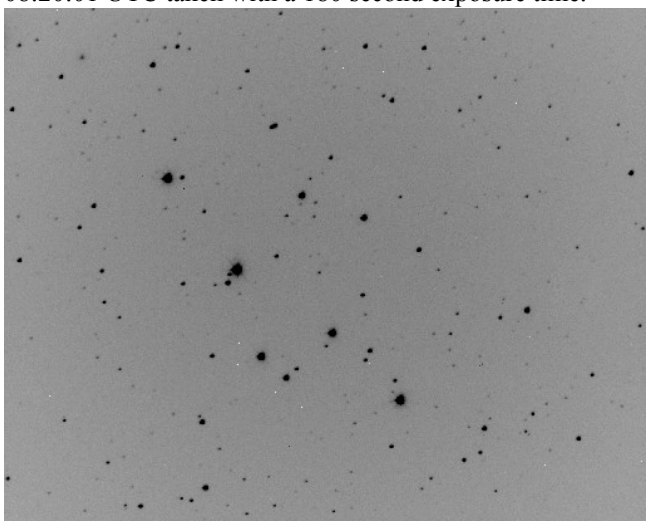

FIGURE 7. Image of 2000 JQ66 on July 23rd, 2016 06:27:31 UTC taken with a 180 second exposure time.

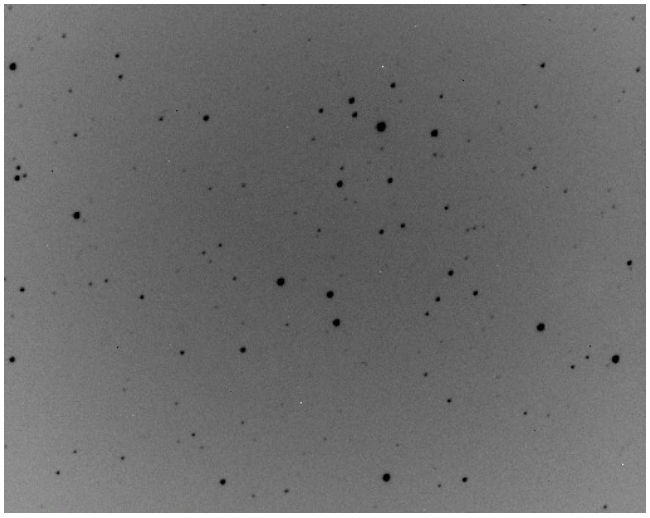

FIGURE 8. Image of 2000 JQ66 on July 27th, 2016 05:26:40 UTC taken with a 180 second exposure time.

Refer to Appendix 5 for the determined classical orbital elements. The elements were calculated by finding an accurate value for r_0 and $\dot{r}_0$ through Gauss' method of orbit determination (Appendix 2). The data calculations were based on the images below (Figures 6-8), taken on July 15th, 2016 08:20:01 UTC, July 23rd, 2016 06:27:31 UTC, and July 27th, 2016 05:26:40 UTC respectively.

We also used data obtained from another team observing 2000 JQ66 at the Summer Science Program to calculate the uncertainty of our own data. Using the Ephemeris Generation program, we calculated the RA and dec of our asteroid at the time of the other team's observation with our calculated orbital elements (refer to Appendix 4 for details). A statistical resampling technique called "jackknifing" was used to see the variations in the orbital elements and further confirm our uncertainty calculations presented in Appendix 5.

The previously accepted values of the orbital elements from JPL Horizons are presented below. Comparison of our calculated values with JPL Horizon's computer elements are presented in Appendix 3.

TABLE 6:

	Semi-major axis (a) [AU]	**Eccen. (e)**	**Inc. (i) [deg]**	**Longitude of Ascending Node (Ω) [deg]**	**Argument of Perihelion (ω) [deg]**	**Mean Anomaly (M)**
JPL Values	2.166	0.4185	7.061	188.97	103.84	5.085

TABLE 6. A table showing the previously accepted values of orbital elements obtained from JPL Horizons.

CONCLUSION

During the five weeks here at the Summer Science Program, the orbit for asteroid 2000 JQ66 was determined with excellent accuracy—proof that science works! Real life observations confirmed the theoretical procedures and programs within the lab. As will all scientific data, analyzing and interpreting the data will provide further insight into our understanding of near-Earth asteroids and their orbit.

Discussion

The data collected confirms the published values from JPL Horizons with uncertainty (refer to Appendix 5). The asteroid's orbital elements demonstrate minimal error, indicating that our determined orbit matches the data from JPL, even though JPL uses a different procedure and algorithm from ours (refer to Appendix 3). Nevertheless, the impact of our analysis of asteroid 2000 JQ66 offers a clearer perspective of the vast multitude of near-Earth

asteroids in space, each of which can pose a significant impact risk to Earth.

Impact Risk

Since the data collected and observations performed match JPL's results, input of our data into JPL's Small-Body Database Browser produced information about the asteroid 2000 JQ66's orbit in relation to Earth's. According to the close-approach data, the minimum distance for the next century occurs in the year 2169, at a length of 0.2941 AU. Thus, 2000 JQ66 does not pose any imminent threat to Earth, as an impact is highly unlikely within the near future.

ACKNOWLEDGEMENTS

Thank you to the faculty at the Summer Science Program for creating an unforgettable research experience. Thank you to Dr. Dubson and Dr. Fallscheer for providing unparalleled lectures in physics, astronomy, and programming. Thank you to Ioana Pleşca, Andrew Bundas, Samuel Holo, and Isabella Sanders for their support and guidance throughout the program.

APPENDIX

Appendix 1

TABLE 1

	Right Ascension (hms, dec)	Declination (dms, dec)	Time (UT, JD)	Mag	SNR
#1	21 33 43.051 21.56227	+13 46 50.90 13.80992	07/15/08:20:01 2457584.83333	17.3	24
#2	21 43 19.613 21.73562	+13 53 13.93 13.81452	07/23/06:27:31 2457592.75002	17.0	27
#3	21 48 29.012 21.80834	+13 32 31.01 13.48258	07/27/05:56:24 2457596.75001	17.0	26

TABLE 1. A table showing the results of our three asteroid observations with right ascension (Epoch 2000.0) in both hms and decimal degrees, declination (Epoch 2000.0) in both dms and decimal degrees, time in both month/day/UT and Julian days, a magnitude estimate to the tenth of a magnitude, and a signal-to-noise ratio value. The asteroid data was submitted to the Minor Planet Center at the Smithsonian Astrophysical Observatory.

The signal-to-noise ratio was calculated by finding the ratio of the power of the desired signal to the power of the background noise:

$$SNR = \frac{P_{signal}}{P_{noise}}$$

The values were then confirmed by processing our CCD images through MaximDL.

Appendix 2

To approximate the values of r_0 and $\dot{r}_0$, we applied Gauss' method of orbit determination, which involves expanding the vector orbital elements as a Taylor series polynomial. The vector r can then be found by finding the "f" and "g" coefficients of the r_0 and $\dot{r}_0$ terms.

$$r(\tau) = fr_0 + g\dot{r}_0$$

Since the vectors r_0 and $\dot{r}_0$ are in the same orbital plane, any position vector r can be expressed as some linear combination of r_0 and $\dot{r}_0$. Using length units of au and time units of Gaussian days, the formula for f-series is given by:

$$1 - \frac{\tau^2}{2{r_0}^3} + \frac{(\vec{r_0} \cdot \dot{\vec{r_0}})\tau^3}{2{r_0}^5}$$

Formula for g-series:

$$\tau - \frac{\tau^3}{6{r_0}^3}$$

With this equation for the vector orbital elements, we begin an iterative process to get more accurate values for r_0 and $\dot{r}_0$.

TABLE 2

	$\mathbf{r_0}$	$\mathbf{\dot{r}_0}$
Initial Guess	(1.040189120, -1.155413349,	(0.926082980, 0.637660239,

	-0.193318705)	0.161167348)
1st Iteration	(0.895056426, -1.057051297, -0.235733581)	(0.906943555, 0.583758388, 0.169988823)
5th Iteration	(0.787595024, -0.984660410, -0.267593805)	(0.887325693, 0.550745385, 0.178262224)
10th Iteration	(0.7726828679, -0.974614903, -0.272014970)	(0.884685604, 0.546111701, 0.179431389)
15th Iteration	(0.770817800, -0.973358508, -0.272567927)	(0.884356811, 0.545531265, 0.179577975)
20th Iteration	(0.770588133, -0.973190945, -0.272641673)	(0.884312985, 0.545453838, 0.179597531)
25th Iteration	(0.770535609, -0.973168412, -0.272651591)	(0.884306789, 0.545443426, 0.179600161)
30th Iteration	(0.770531105, -0.973165378, -0.272652926)	(0.884306298, 0.545442024, 0.179600515)
35th Iteration	(0.770530499, -0.973164970, -0.272653106)	(0.884306191, 0.545441835, 0.179600565)
40th Iteration	(0.770530417, -0.973164915,	(0.884306178, 0.525441810,
	-0.272651299)	0.1796005683)
45th Iteration	(0.770530406, -0.973164907, -0.272653133)	(0.884306175, 0.545441807, 0.179600570)
46th Iteration	(0.770530406, -0.973164907, -0.272653133)	(0.884306175, 0.545441807, 0.179600570)

TABLE 2. A summary table showing the iterated r_0 and $\dot{r}_0$ from the f and g series. The iterations show sufficient convergence to 9 decimal places after 45 iterations.

Appendix 3

TABLE 3

	Semi-major axis (a) [AU]	**Eccen. (e)**	**Inc. (i) [deg]**	**Longitude of Ascending Node (Ω) [deg]**	**Argument of Perihelion (ω) [deg]**	**Mean Anomaly (M)**
Calc.	2.165	0.4186	7.085	189.10	103.51	5.539
JPL	2.166	0.4185	7.061	188.97	103.84	5.085
Error	4.62%	2.39%	0.67%	3.61%	9.17%	12.61%

TABLE 3. A table comparing the calculated six orbital elements (semi-major axis, eccentricity, longitude of ascending node, argument of perihelion, and mean anomaly) to JPL Horizon's computer elements [6]. The last row shows the error between our values and Horizon's values. The error for semi-major axis (a) and eccentricity (e) are calculated with a straightforward percentage, and the other orbital elements are calculated with an adjusted percent error:

$$error = \frac{CalculatedAngle - Horizon'sAngle}{2\pi}$$

Appendix 4

The following data was obtained from another team observing 2000 JQ66 at the Summer Science Program. Their observations were used in calculating the uncertainty of our own data by statistical resampling. The team consists of Brin Harper, Olivia Durrett, and George Sabatakakis. We obtained the RA, Dec, and time of a mid-point observation of an image from the other team. Then, using the ephemeris generation program, we input our orbital elements to compute the RA and Dec of 2000 JQ66 from their observation time.

TABLE 4.

	Time (UT, JD)	Right Ascension (hms, dec)	Declination (dms, dec)
Comp.	07/23/08:20 2457592.847	21 48 35.10 21.80975	+13 28 19.2 13.47219
Actual	07/23/08:20 2457592.847	21 44 13.08 21.73697	+13 48 37.2 13.81033

TABLE 4. A table showing the computed values of RA and Dec from the ephemeris generation program and the data obtained by the other team.

Appendix 5

To determine the uncertainty estimates, the CCD images were processed through the Least-Squares Plate Reduction program to figure out the standard deviation of the asteroid's RA and Dec. After adjusting the RA and Dec with the computed deviation, the data was run through the orbit determination program to determine the adjusted classical orbital elements. The difference between adjusted and calculated orbital elements was then used to determine the total estimate for uncertainty for each orbital element using the following formula:

$$\sigma_e = \sqrt{\sum_i^n {\sigma_i}^2}$$

σ_e represents the estimate of uncertainty for a certain orbital element and σ_i is the difference between the adjusted and calculated orbital elements determined by the orbit determination program. This procedure's results for uncertainty were confirmed through a statistical resampling technique with the other team's observational data.

TABLE 5

Quantity	Value	Uncertainty
Semi-major axis (a)	2.164660 AU	0.004523 AU
Eccentricity (e)	0.4186375	0.0004642
Inclination (i)	7.084588 degrees	0.02865 degrees
Longitude of Ascending Node (Ω)	189.1004 degrees	0.4818 degrees
Argument of Perihelion (ω)	103.5142 degrees	0.4787 degrees
Mean Anomaly (M)	5.538538	0.9752

TABLE 5. A table portraying the values of the classical orbital elements calculated as well as the total estimate of uncertainty. The data was compared with the published values from JPL Horizons.

[1] *Hoskin, Michael (26 June 1992). "Bode's Law and the Discovery of Ceres". Observatorio Astronomico di Palermo "Giuseppe S. Vaiana". Retrieved* 30 *July 2016.*

[2] *"What Are Asteroids And Comets?". Near Earth Object Program FAQ. NASA. Retrieved* 30 July *2016.*

[3] Tedesco, Edward; Metcalfe, Leo (4 April 2002). "New study reveals twice as many asteroids as previously believed" (Press release). European Space Agency.

[4] www.nasa.gov/missionpages/asteroids/overview/fastfacts.html Retrieved 30 July 2016

[5] http://nineplanets.org/asteroids.html Retrieved 30 July 2016.

[**6**] http://ssd.jpl.nasa.gov/sbdb.cgi Retroeved 30 July 2016.

[**7**] http://ssd.jpl.nasa.gov/?horizons, retrieved 7/30/2016.